CrossMark

Mesenchymal Stem Cells from Nucleus Pulposus and Neural Differentiation Potential: a Continuous Challenge

Raffaella Lazzarini[1] · Simone Guarnieri[2] · Gianluca Fulgenzi[3] · Maria Addolorata Mariggiò[2] · Laura Graciotti[3] · Monia Martiniani[4] · Monia Orciani[1] · Nicola Specchia[4] · Roberto Di Primio[1]

Abstract

Mesenchymal stem cells (MSCs) are well-characterized adult stem cells, recently isolated from human nucleus pulposus of degenerate and non-degenerate intervertebral disc. The attention to this source is linked to its embryologic history and cells may conserve a stronger aptitude to neuronal differentiation than other MSCs. Here, MSCs from nucleus pulposus (NP-MSCs) were successfully isolated and characterized for morphology, proliferation, and expression of selected genes. Subsequently, the neuronal differentiation was induced by 10 days of culture with a neuronal medium. NP-MSCs subjected to neural differentiation media (NP-MSCs-N) showed a morphological and biochemical modifications. NP-MSCs-N displayed elongated shape with protrusion, intermediate filaments, microtubules, and electron dense granules and the ability to form neurospheres. Even if they expressed neural markers such as NESTIN, β-TUBULIN III, MAP-2, GAP-43, and ENOLASE-2, the neural differentiated cells did not show neither spontaneous nor evoked intracellular calcium variations compared to the undifferentiated cells, suggesting that cells do not have electric functional properties. Further studies are required in order to get a better understanding and characterization of NP-MSCs and analyzed the molecular mechanisms that regulate their neural differentiation potential.

Keywords Nucleus pulposus mesenchymal stem cells · Neural differentiation · Regenerative medicine

Introduction

Mesenchymal stem cells (MSCs) were classified as a heterogeneous non-hematopoietic, plastic-adherent population of cells that can be differentiated in vitro into cells of osteogenic, chondrogenic, adipogenic, myogenic, and other lineages (Ullah et al. 2015).

✉ Monia Orciani
m.orciani@univpm.it

1   Department of Clinical and Molecular Sciences - Histology, Università Politecnica delle Marche, 60126 Ancona, Italy

2   Department of Neuroscience, Imaging and Clinical Sciences and Centro Scienze dell' Invecchiamento e Medicina Traslazionale (CeSI-MeT), "G. d'Annunzio" University of Chieti-Pescara, 66100 Chieti, Italy

3   Department of Clinical and Molecular Sciences – Pathology, Università Politecnica delle Marche, 60126 Ancona, Italy

4   Department of Clinical and Molecular Sciences – Clinic of Orthopaedics, Università Politecnica delle Marche, 60126 Ancona, Italy

Originally isolated from bone marrow (Friedenstein et al. 1968), today it is well accepted that almost every adult tissue has a reserve of stem cells (Bianco et al. 2008; Sagar et al. 2018; Zannettino et al. 2008; Orciani et al. 2015; Lazzarini et al. 2014; Orciani et al. 2010; Foudah et al. 2014).

Suggested minimal criteria to define human MSC were published in 2006 by Dominici et al. (2006). These criteria included that MSCs isolated from different sources do not express CD45, CD34, and CD14 or the co-stimulatory molecules CD80, CD86, and CD40, whereas they express variable levels of CD105 (also known as endoglin), CD73 (ecto-5′nucleotidase), CD44, CD90 (THY1), CD71 (transferrin receptor), the ganglioside GD2, and CD271 (low-affinity nerve growth factor receptor), and they are recognized by the monoclonal antibody STRO-1. The variation observed in the expression levels of these stem cells markers depends on the species differences, tissue sources, and culture conditions (Uccelli et al. 2008).

MSCs have been extensively studied due to their ability of self-renewal and differentiation into mature cells of mesodermal and non-mesodermal origin (Pittenger et al. 1999). In

addition, MSCs are able to promote wound healing and regeneration of surrounding tissues by modulating immune and inflammatory responses, promoting angiogenesis and secreting other trophic factors; for these reasons, they have been used for cell replacement, repair, and regeneration (Madrigal et al. 2014).

In particular, neurodegenerative and acute neurological pathologies represent a critical issue in clinical research, since no complete recovery of central nervous system (CNS) functionality can be achieved in many diseases. In adults, only restricted brain areas still house cells competent to generate newborn neurons (Zhao et al. 2008; Casarosa et al. 2014); the subsequent limited neurogenesis does not seem to be sufficient to enable neuronal regeneration in cases of traumatic, ischemic, or degenerative damages of the CNS. Interestingly, MSCs display an intrinsic neuronal potential and ability to differentiate into neural cell phenotypes, both in vitro *and* in vivo (Alexanian et al. 2008).

In addition, several studies reveal that implanted MSCs could incorporate into the injured spinal cord and display the tendency to migrate toward insulted area raising the hope for developing new therapeutic strategies for CNS damage repair (Shyu et al. 2007). Furthermore, in case of injury, MSCs inhibit fibrotic remodeling and apoptosis, stimulate endogenous stem cell recruitment and proliferation, and reduce immune responses (Uccelli et al. 2011; Trueman et al. 2013).

Recently, Blanco et al. (2010) and Shen et al. (2015) reported the isolation of MSCs from the degenerate and not degenerated human nucleus pulposus-derived mesenchymal stem cells (NP-MSCs), respectively.

Compared with BM-MSCs, NP-MSCs show a quite similar morphology, expansion potential, immunophenotypic and molecular profile, as well as differentiation ability. The interest about NP-MSCs depends on the hypothesis that these cells could more easily differentiate toward neuronal lineage: the nucleus pulposus of the intervertebral discs is a postembryonic vestige of the notochord that forms during gastrulation and soon after induces the formation of the neural plate (neurulation), synchronizing the development of the neural tube.

In this work, MSCs were isolated from nucleus pulposus, characterized, and induced toward neuronal differentiation; MSCs from amniotic fluid (AF-MSCs), considered as intermediate between embryonic and adults MSCs and for this reason with higher differentiative potential, were used for comparative purposes during the characterization.

Material and Methods

Sample Collection

The local Ethics Committee of Università Politecnica delle Marche approved all procedures performed for the present

work; five samples of nucleus pulposus were collected after informed consent from patients who underwent to discectomy, preserving patient anonymity. The nucleus pulposus (NP) tissues were carefully separated from the annulus fibrous using surgical loupes, in order to avoid contamination by annulus fibrous or any other tissue. The age of the donors was 54 ± 4, and the five patients were all male. Human amniotic fluid samples (AF, no. 3) were obtained from amniocentesis as previously described (Lazzarini et al. 2014).

Isolation of MSC from NP

NP tissue was both mechanically fragmented and subjected to enzymatic digestion with 0.2% type II collagenase (Sigma-Aldrich, Milan, Italy) at 37 °C for 4 h. The partially digested tissue was cultured in the DMEM F12 (EuroClone, Milan, Italy) medium, supplemented with 10% fetal bovine serum (FBS), 1% L-glutamine, and 1% penicillin-streptomycin (EuroClone, Italy). Twice a week, adherent cells were fed by complete replacement of the medium. Cells were maintained in culture until they reached 80% confluence. Cells were used only when no major abnormalities were revealed by cytogenetic analysis. Cell morphology was evaluated by phase-contrast microscopy (Leica DM IL; Leica Microsystem GmbH, Wetzlar, Germany). AF-MSCs were isolated and characterized as previously described (Lazzarini et al. 2014). All the subsequent experiments were performed with cells at third and sixth passages.

(4,5-Dimethylthiazol-2-yl)-2,5-diphenyltetrazolium bromide assay and doubling time

Cell viability of AF- and NP-MSCs was evaluated by a (4,5-dimethylthiazol-2-yl)-2,5-diphenyltetrazolium bromide (MTT) assay as previously described (Mariotti et al. 2015). Briefly, 2.5×10^3 cells were seeded onto 96-well plates, and every day up to 6 days, MTT (Sigma-Aldrich, Milan, Italy) was added. All tests were performed in triplicate and the OD values were expressed as mean ± SD. The doubling time was calculated from passage 1 to passage 14 as previously described (Mariotti et al. 2015).

Analysis of Cellular Phenotype and Differentiation Potential of NP-MSCs

For immunophenotyping analysis, NP-MSC cells at third passage and sixth passage were examined by multiparameter flow cytometry (MFC, FACSCanto II BD Biosciences). MFC immunophenotypic studies were performed with the following monoclonal antibody combination: in the first tube: CD90-FITC, CD105-PE, human leukocyte antigen (HLA)-DR-PCP, CD34-PECy7, CD14-APC, and CD45-APC-Cy7; in the other tube: CD73-PE, CD19-PCP, CD13-PECy7, and

CD11b-APC. In the logarithmic phase of growth, NP-MSCs were detached and 2.5×10^5 cells/tube used for MFC analysis. Briefly, cells were washed with PBS, incubated with antibody for 20 min, in the dark at room temperature. Thereafter, the cells were rinsed with PBS, centrifuged, and re-suspended with 200 μl of PBS for flow cytometry analysis (FACSDiva Software). Cells were analyzed in triplicate for each antigen phenotype. Differentiation in osteocytes, chondrocytes, and adipocytes was assessed using StemPro Osteogenesis, Chondrogenesis, and Adipogenesis kits (GIBCO, Thermo Fisher, Waltham, MA, USA), respectively. Cells cultured in DMEM-F12 were used as a negative control. Osteogenic differentiation was assessed by von Kossa staining and alkaline phosphatase (ALP) reaction; adipogenic differentiation was tested by Oil Red staining. For chondrogenic differentiation, a pellet culture was employed, and sections were exposed to a solution of Safranin O and Alcian Blue.

Quantitative PCR (Real-Time PCR)

Total RNA was isolated from NP-MSCs and AF-MSCs at third and sixth passages using PerfectPure RNA Cell and Tissue (5 PRIME, Hamburg, Germany) following the manufacturer's instructions. RNA was measured to determine the 260/280-nm absorbance ratio (≥ 1.9) using a spectrophotometer (Nanodrop, EuroClone, Milan, Italy) and treated with RNase-free DNase prior to reverse transcription into cDNA. One microgram of total RNA was reverse-transcribed with GoScript Reverse Transcription System (Promega, Milan, Italy). Real-time PCR analysis was performed using EVA Green PCR Master Mix (Bio-Rad, Milan, Italy) and a Master Cycle (Eppendorf, Milan, Italy) instrument. All samples were tested in triplicate with the reference genes GAPDH and β-ACTIN for data normalization. One of the two, GAPDH, gave the most consistent results and was therefore used. After amplification, melting curves were acquired. All primers were synthesized by Sigma Genosis (Sigma-Aldrich, Milan, Italy). The primer sequences of genes related to stemness (SOX2, KLF4, NANOG, OCT4) are reported in Table 1. The mRNA expression levels were calculated by the $2^{-\Delta\Delta Ct}$ method, $\Delta (\Delta Ct) = \Delta Ct$ (NP-MSCs) $- \Delta Ct$ (AF-MSCs) and $\Delta (\Delta Ct) = \Delta Ct$ (NP-MSCs) $- \Delta Ct$ (NP-MSCs-N).

In addition, the expression of genes specifically expressed by NP, such as aggrecan (ACAN), collagen type I (COL1A1), collagen type II (COL2A1), cartilage oligomeric matrix protein (COMP), SOX6, and SOX9, was analyzed. Quantification of mRNA expression levels in NP-MSCs was calculated with the $2^{-\Delta Ct}$ method, where Ct is the parameter threshold cycle, $\Delta Ct = Ct$ (gene of interest) $- Ct$ (control genes). Primer sequences are reported in Table 1.

The values of the relative expression of genes of interest are given as mean $\pm$ SD, over three independent experiments.

Neural Differentiation of NP-MSCs

Neural differentiation was induced in cells both at third and sixth. NP-MSCs were seeded a 1×10^5/ml into six-well cell culture plates; when the cells achieved 70–80% confluency, neural medium was added to cells.

Neural medium was prepared using DMEM-F12, supplemented with B27 (Gibco, Milan, Italy), 1% penicillin/streptomycin (EuroClone), 20 ng/ml fibroblast growth factor-basic (FGF-basic; PeproTech, R&D, Milan, Italy), 20 ng/ml epithelial growth factor (EGF, PeproTech), and 50 ng/ml insulin-like growth factor (IGF, PeproTech). Cells cultured in control medium (CTRL, DMEM-F12 + 10% FBS) were used as a negative control.

Cells were cultured for 10 days. Morphological changes, MTT assay, doubling time, and expression of the genes referred to stemness, to chondrogenesis, and to neurogenesis (β-TUBULIN III and NESTIN, primer sequences in Table 1) were assessed in NP-MSCSs, before and after neural differentiation (NP-MSCs-N) for comparative analysis. To better analyze morphological changes after 10 days of neuronal induction, cells were fixed in 4% PFA for 30 min, washed twice with PBS, and stained with hematoxylin solution for 10 min, then washed with tap water, rinsed in distilled water, and mounted using a water-based mounting media.

Neurosphere Formation

To test the ability to form neurosphere, NP-MSCs were cultured in a low adherence condition with CTRL medium or Neuro Basal Medium (Gibco, Milan, Italy), 1% B27 (Gibco), 1% penicillin-streptomycin, 1% L-glutamine, 20 ng/ml FGFb, and 20 ng/ml EGF. Every day, half of the culture medium was replaced with fresh one avoiding disturbance of the floating cells. After 10 days, the spheres were collected, digested, and re-plated either in low adherence or glass chamber slide to test the self-renewal and the neural differentiation capabilities. Images were taken using a Nikon 80i microscope equipped with fluorescence unit and a camera connection.

Western Blot Analysis

Proteins were extracted from NP-MSCs before and after neural differentiation. Radio immunoprecipitation assay buffer [150 mM NaCl, 10 mM Tris (pH 7.2), 0.1% sodium dodecyl sulfate, 1.0% Triton X-100, and 5 mM ethylenediaminetetraacetic acid (pH 8.0)] containing protease inhibitor cocktail (Roche Applied Science, Indianapolis, IN, USA) was used for protein extraction. Protein concentration was determined using Bradford reagent (Sigma-Aldrich). Total protein extracts (40 μg) were reduced in dithiothreitol (DDT, 0.5 M) for 10 min at 70 °C and samples run on a 4–12% gradient

Table 1 Primer sequence

Gene	Primer forward	Primer reverse
NANOG	TGAACCTCAGCTACAAACAG	CTGGATGTTCTGGGTCTGGT
OCT4	AGCGAACCAGTATCGAGAAC	GCCTCAAAATCCTCTCGTTG
SOX2	AGCTACAGCATGATGCAGGA	GGTCATGGAGTTGTACTGCA
KLF4	CCCACACAGGTGAGAAACCT	ATGTGTAAGGCGAGGTGGTC
ACAN	GTGCCTATCAGGACAAGGTCT	GTGCCTATCAGGACAAGGTCT
COL1A1	GTGCCTATCAGGACAAGGTCT	CAGATCACGTCATCGCACAAC
COL2A1	TGGACGCCATGAAGGTTTTCT	TGGACGCCATGAAGGTTTTCT
COMP	GATCACGTTCCTGAAAAACACG	GATCACGTTCCTGAAAAACACG
SOX6	GGATGCAATGACCCAGGATTT	TGAATGGTACTGACAAGTGTTGG
SOX9	AGCGAACGCACATCAAGAC	CTGTAGGCGATCTGTTGGGG
NESTIN	CAATCCCTGCAAAAGGAGAA	CAATCCCTGCAAAAGGAGAA
β-TUBULIN III	CATGGACAGTGTCCGCTCAG	CAGGCAGTCGCAGTTTTCA
β-ACTIN	GGACTTCGAGCAAGAGATGG	GATGGAGTTGAAGGTAGTTTCG
GAPDH	AGCCACATCGCTCAGACAC	GCCCAATACGACCAAATCC

precast NuPAGE Bis–Tris polyacrylamide gel for 1 h at 200 V. Electroblotting was performed using the iBlot Dry Blotting System (Thermo Fisher, Milan, Italy). Membranes were incubated overnight with primary antibodies anti-NESTIN (1:1000, Biorbyt, Cambridge, UK), anti-ENOLASE-2 (1:1000, Cell Signaling Technology (Danvers, MA, USA), anti-SNAP25 (1:1000, Serotec Ltd., Oxford, UK), and anti-VAMP2 (1:1000, Synaptic System, Goettingen, Germany) followed by incubation with a secondary antibody conjugated to horseradish peroxidase (Santa Cruz Biotechnology, CA, USA) for 1 h at room temperature. Immunoreactive proteins were visualized using chemiluminescence substrate (Santa Cruz Biotechnology), followed by densitometric analysis. As loading controls, the membrane was incubated with anti-β-actin (Santa Cruz Biotechnology).

Confocal Laser Scanning Microscope Analysis (CLSM)

Control and differentiated NP-MSCs cells were grown on 12-mm glass coverslip and fixed for 10 min at room temperature (RT) with 4% of paraformaldehyde in 0.1 M sodium phosphate-buffered saline (PBS), pH 7.4, and permeabilized with 0.1% of Triton X-100 in PBS for 10 min, followed by blocking with 10% goat serum in PBS for 60 min. Samples were incubated overnight at 4 °C with the following primary mouse antibody: mouse anti-NESTIN dil. 1:100, mouse anti-β-TUBULIN III (dil. 1:100, Santa Cruz Biotechnology), mouse anti-ENOLASE-2 (dil. 1:100, Santa Cruz Biotechnology), mouse anti-microtubule-associated protein 2 (MAP-2) (dil. 1:100, Santa Cruz Biotechnology), and rabbit anti-GAP-43 (dil. 1:100, Santa Cruz Biotechnology). The secondary antibodies, goat anti-mouse Alexa Fluor 488, and anti-rabbit Alexa Fluor 568 (Molecular Probes, Life Technologies, Monza,

MI, Italy) were used for green and red emission, respectively. After secondary incubation (2 h, RT), samples were incubated with DAPI (Molecular Probes) diluted 1:100, to highlight the nuclei. The glass coverslips were placed upside down on glass slides and mounted with ProLong antifade (Molecular Probes) (Caprara et al. 2016).

TEM and SEM

Cells were plated on ACLAR and cultured at 1×10^5 cells/cm^2 (Ted Pella CA, USA); chips were trimmed to fit into the multiwell plates. The ACLAR insets were sterilized just before use. Cells were grown with control and neural medium, and medium was changed every 3 days. After 7 and 10 days of culture, cells were fixed with glutaraldehyde 2% in 0.1 M cacodylate buffer pH 7.0, for 1 h at room temperature and subsequently overnight at 4 °C. For TEM, cells were postfixed in 1% osmium tetroxide for one additional hour, then dehydrated with acetone series and flat embedded in Luft epoxy resin using a polystyrene capsule. After hardening of the resin, ACLAR was peeled off and ultrathin sections (50 nm) obtained.

The sections were stained with uranyl acetate alcoholic solution and lead citrate then imaged at 80 K volts in a Philips CM12 electron microscope. For SEM, after fixation, cells were dehydrated in ethyl alcohol series and then processed for critical point drying. ACLAR chips mounted on aluminum stubs were coated with gold and imaged in a Philips XL20 at 15 K volts microscope.

Measurement of Intracellular Ca^{2+} in Single Cells

The [Ca2+]i was measured using the dye fluo-4-acetoxymethyl ester (Fluo-4/AM; Molecular Probes),

using an upright Zeiss Axio Examiner (Carl Zeiss, Jena, Germany) equipped with ×40 0.75NA water immersion objectives. The microscope is connected by an optical fiber to a 75-W xenon lamp of galvomonchromator (OptoScan, Cairn Instrument, England, UK) with submillisecond band-pass and wavelength controls. For the experiments, the control and differentiated NP-MSCs were plated on a 25-mm glass coverslip into a six-well plate (Sigma-Aldrich), and at selected time, the coverslips were transferred in a 35-mm plastic dish and incubated with 5 μM Fluo-4/AM for 30 min at 37 °C in normal external solution (NES, in mM: 140 NaCl, 2.8 KCl, 2 CaCl$_2$, 2 MgCl$_2$, 10 glucose, 10 N-2-hydroxyethilpiperazione-N'-2-ethanesulfonic acid (HEPES)-NaOH, pH 7.3) plus 1% (w/v) of bovine serum albumin. Fluo-4/AM-loaded cells were recorded on NES excited at 488 nm and the emitted fluorescence was acquired by back-illuminated EMCCD Evolve 512 (Photometrics, Tucson, AZ, USA). Images were captured at 4 frame/s stored on an interfaced computer for offline analysis. The temporal analysis was calculated as mean fluorescence intensity signal in selected cell areas as $F/F0$, where F is the fluorescence emission of a single-loaded cell acquired during a time lapse and $F0$ is the mean fluorescence intensity value of the same cell calculated from all images acquired during the first 10 s. To evaluate the effect of depolarization, the cells were bathed with NES plus 50 mM KCl (Morabito et al. 2010).

Statistical Analysis

Statistical analysis was performed by using SPSS 19.0 software (SPSS, Inc., Chicago, IL, USA). All data are presented as mean ± SD. Statistical significance was calculated for two-sample comparisons by Student's t test using SPSS 17.0 software. Statistical significance was analyzed for data from at least three independent experiments. P values ≤ 0.05 were defined as significant.

Results

Isolation, Culture, and Characterization of NP-MSCs

NP-MSCs were isolated from five samples; these cells exhibited the same spindle-shaped morphology, typical of the mesenchymal stem cells. NP-MSCs maintained a quite similar morphology from the first passage up to third and sixth passages (9 and 18 days of culture, respectively (Fig. 1a, b). AF-MSCs, used as a control, maintain a similar fibroblastoid morphology (passage 3, Fig. 1c). NP-MSCs at third and sixth passages were analyzed by

flow cytometry and 97% of the tested cells co-expressed CD105, CD90, CD13, and CD73 but not CD34, CD19, CD14, CD11b, CD45, and histocompatibility antigen HLA-DR (major histocompatibility complex class II) (Fig. 1d). A small portion (3%) of tested cells at third passage co-expressed CD90 and CD13 but not CD73, CD34, CD19, CD45, and histocompatibility antigen HLA-DR; this cell population was no more detectable in cells at sixth passage. For cell viability, MTT assay was performed for six consecutive days; DT was calculated from passage 1 up to passage 14. Growth rate and viability of NP-MSCs were comparable to those observed for AF-MSCs, as shown in Fig. 1e, f.
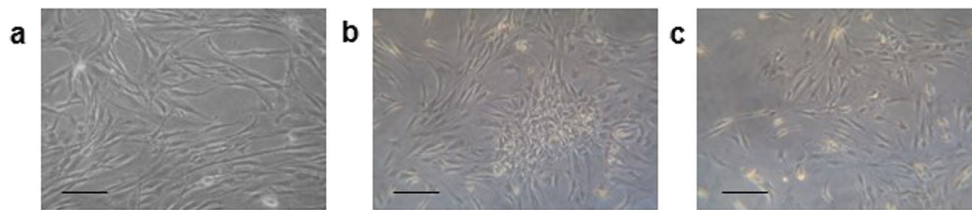
The expression of the genes related to stemness (NANOG, SOX2, KLF4, and OCT4) or referred specifically to NP and to chondrogenic tissue (COL1A1, COL2A2, ACAN, COMP, SOX9, and SOX6) was tested by RT-PCR in NP-MSCs and AF-MSCs at third and sixth passages. Since the number of passage did not affect the expression levels that remain stable, only histograms referred to cells at passage 3 are reported. For stemness genes, NP-MSCs showed a significant higher expression of OCT4 than AF-MSCs, while NANOG, SOX2, and KLF4 were downregulated compared to AF-MSCs (Fig. 2a). A decrease in their expression was observed after 10 passages (data not shown). For genes referred specifically to NP and to chondrogenic tissue, their expression was glaring in NP-MSCs (Fig. 2b) and very low or undetectable in AF-MSCs (data not show).

Under mesenchymal differentiation condition, like observed for AF-MSCs (Lazzarini et al. 2014), NP-MSCs were able to differentiate in osteogenic (Fig. 2c, d) and chondrogenic lineages (Fig. 2e, f) but failed to differentiate into adipocytes (data not shown).

### Morphology and Proliferation After Neural Differentiation

NP-MSCs at passage 3 or 6 were transferred to neural differentiation medium (NP-MSCs-N) and analyzed after 10 days of culture. NP-MSCs cultured in non-differentiating medium at the same passage were used as control. Since no differences were noted between NP-MSCs-N at passage 3 and at passage 6, here only results obtained from NP-MSCs-N cells started at passage 3 were reported.

After 10 days of differentiation, an increased number of neural-like cells displaying small oval cell body with extended protrusion was identified by using an optical microscope. Undifferentiated NP-MSCs maintained the fibroblast-like spindle-shaped morphology. Hematoxylin staining of NP-MSCs-N highlights the morphological changes of NP-MSCs-N compared to undifferentiated

Marker	% stained cells	No events
CD105	+96.7±1.8	10.000
CD90	+93.8±2.1	10.000
CD73	+90.3±1.3	10.000
CD13	+82.6±3.1	10.000
CD34	-95.1±1.1	10.000
CD45	-89.2±0.4	10.000
CD14	-96.7±0.8	10.000
CD19	-82.6±4.1	10.000
CD11b	-87.5±2.9	10.000
HLA-DR	-96.1±0.81	10.000
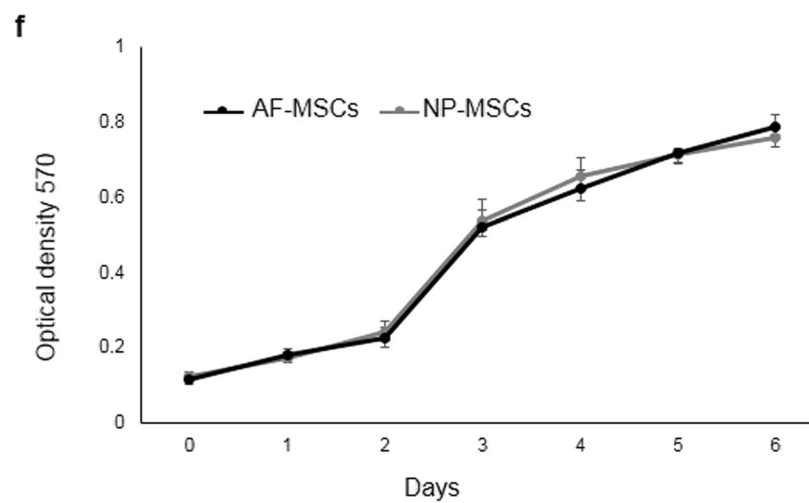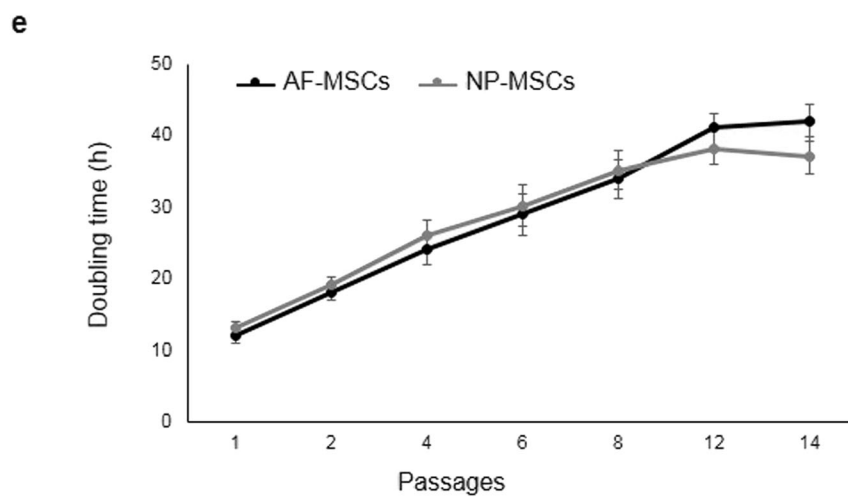
◄ **Fig. 1** Morphology, immunophenotype, and proliferation of MSCs derived from nucleus pulposus (NP-MSCs). Phase-contrast images of NP-MSCs cells after 9 days (**a**) and 18 days (**b**) of culture. AF-MSCs after 9 days of culture (**c**). Scale bar 100 μm. **d** Immunophenotype of NP-MSCs. Data reported are representative of experiment performed on five samples of NP-MSCs, at third and sixth passages. No evident differences were noted among samples. **e** Doubling time analysis from 1st to 14th passages of NP-MSCs and AF-MSCs. **f** MTT assay of AF-MSCs and NP-MSCs for 6 days. Data reported (mean ± SEM) are representative of independent experiments performed on three samples of AF-MSCs and five samples of NP-MSCs. AF-MSCs, mesenchymal stem cells derived from amniotic fluid; NP-MSCs, mesenchymal stem cells derived from nucleus pulposus
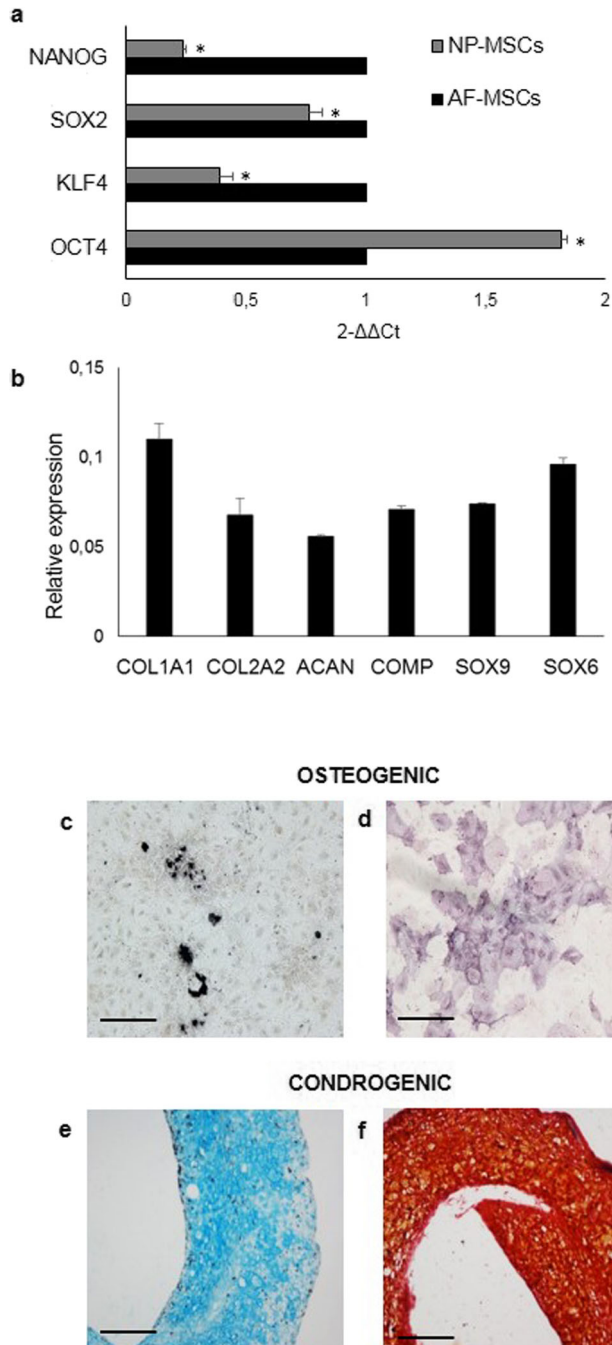
NP-MSCs (Fig. 3a). In addition, NP-MSCs cultured in a low adherence condition were able to form neurospheres after 10 days of neural induction (Fig. 3b) where undifferentiated NP-MSCs failed (Fig. 3b).

Neural differentiation produced a decrease of the proliferation rate and viability of NP-MSCs-N with respect to NP-MSCs, as identified by population doubling time (Fig. 3c) and MTT test (Fig. 3d).

Analysis by RT-PCR of the Expression of Selected Genes After Neural Differentiation

For stemness genes, NP-MSCs-N showed an upregulation of SOX2 and NANOG expression compared to undifferentiated cells, while no significant differences were identified for OCT4 and KLF4 genes (Fig. 4a). Among NP-specific genes, COMP, SOX9, and SOX6 were less expressed in NP-MSCs-N than NP-MSCs; no differences were identified for the COL1A1 and ACAN and finally the expression of COL2A1 was higher in NP-MSCs-N than in undifferentiated cells (Fig. 4b). For genes related to neurogenesis, NESTIN and β-TUBULIN III were overexpressed by NP-MSCs-N compared to NP-MSCs cells, but this increase was statistically significant only for NESTIN (Fig. 4c).

Analysis by WB of the Expression of NESTIN, ENOLASE-2, SNAP25, and VAMP2 After Neural Differentiation

The expression of NESTIN, ENOLASE-2, SNAP25, and VAMP2 was tested by Western blot followed by densitometric analysis (Fig. 5). All proteins were detectable in NP-MSCs both before and after neural induction, while the expression of NESTIN and ENOLASE-2 was significantly higher in neural differentiated NP-MSCs than control cells ($p < 0.05$); the

◄ **Fig. 2** Gene expression and differentiative potential of NP-MSCs. **a** Analysis of the expression of genes related to stemness (NANOG, SOX2, KLF4, OCT4) by real-time PCR in NP-MSCs at passage 3; the gene expression ratio is reported as fold change respect to AF-MSCs at the same culture passage (expressed equal to 1). Data reported (mean ± SEM) are representative of independent experiments performed on three samples of AF-MSCs and five samples of NP-MSCs; *$p < 0.05$. AF-MSCs, mesenchymal stem cells derived from amniotic fluid; NP-MSCs, mesenchymal stem cells derived from nucleus pulposus. **b** Expression level of mRNA related to NP and chondrogenic specific genes (COL1A1, COL2A2, ACAN, COMP, SOX9, and SOX6). Data reported (mean ± SEM) are representative of independent experiments performed on three samples of AF-MSCs and five samples of NP-MSCs. No expression was detected on AF-MSCs. Lineage differentiation potential of NP-MSC samples using phase-contrast microscopy: osteogenic differentiation by von Kossa staining (**c**; scale bar, 250 μm) and alkaline phosphatase activity (**d**; scale bar, 200 μm), chondrogenic differentiation by Alcian Blue (**e**; scale bar, 500 μm), and Safranin staining (**f**; scale bar, 500 μm). Images are representative of five NP-MSC samples

Fig. 3 Morphology and proliferation rate after neural differentiation. **a** Representative images after hematoxylin staining of NP-MSCs and NP-MSCs-N. **b** Phase-contrast images of NP-MSCs and NP-MSCs-N after 10 days of treatment with neurosphere formation culture medium. Images are representative of three experiments. **c** Doubling time analysis from first to tenth passages and **d** proliferation rate by MTT assay of NP-MSCs and NP-MSCs-N. Data reported (mean ± SEM) are representative of three experiments. NP-MSCs, mesenchymal stem cells derived from nucleus pulposus; NP-MSCs-N, mesenchymal stem cells derived from nucleus pulposus after neuronal differentiation
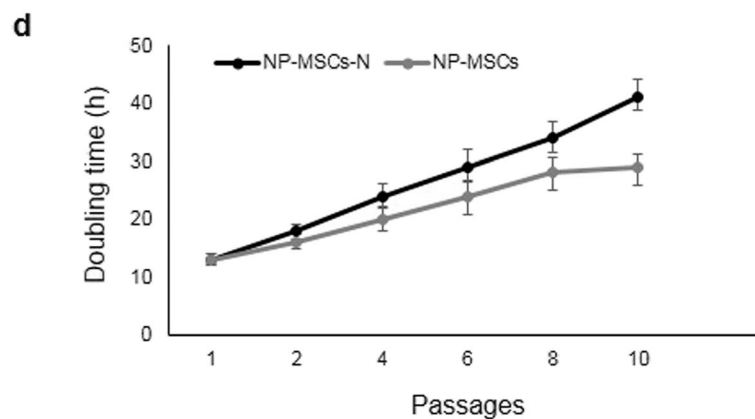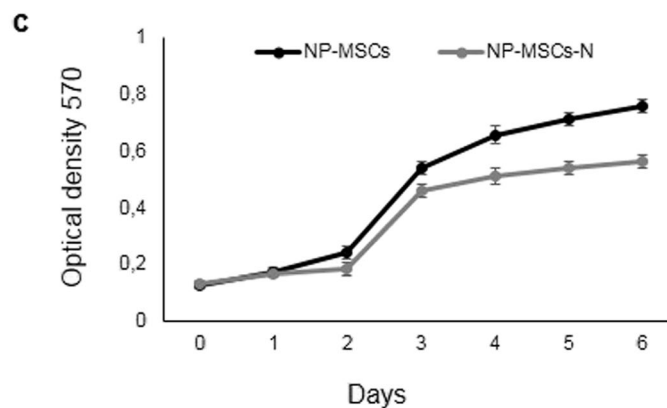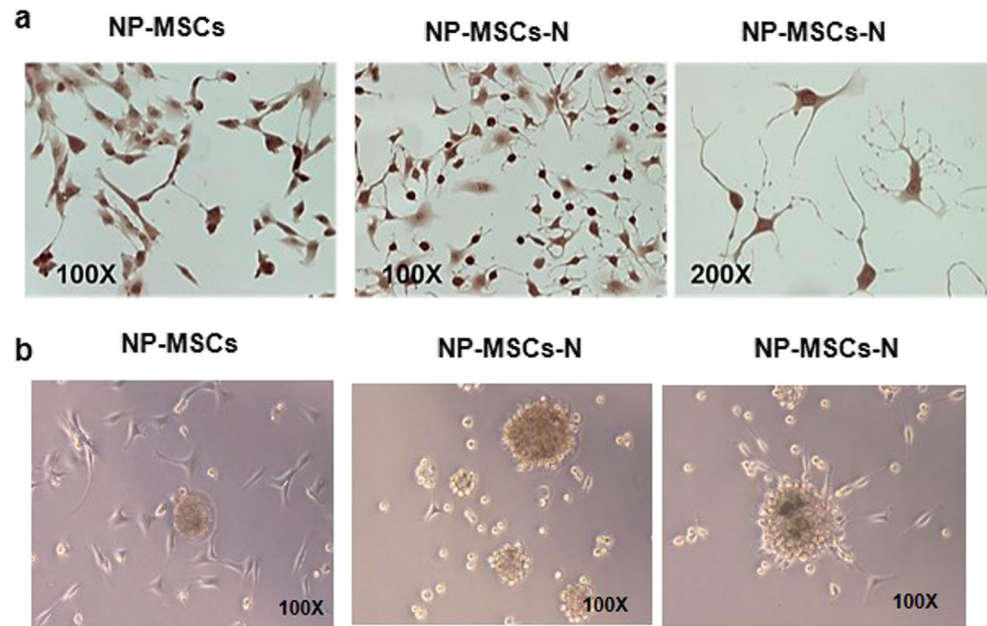
increased expression observed for SNAP25 and VAMP2 in differentiated NP-MSCs does not reach statistical relevance ($p = 0.056$). To note that for NESTIN a reactive band of 100 kDa (instead of 270 kDa) was visualized in each sample, this smaller molecular weight may be due to a cleavage by lysate cryoconservation (Sana et al. 2011).
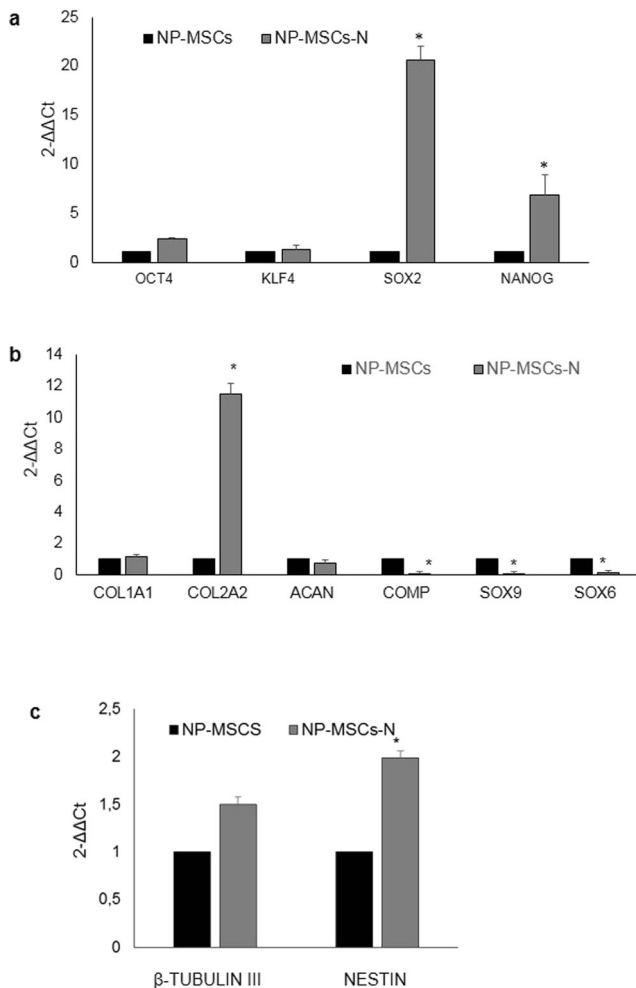
Fig. 4 Gene expression after neural differentiation. Analysis of the expression of genes related to stemness (NANOG, SOX2, KLF4, OCT4) (**a**), to NP and chondrogenic tissue (COL1A1, COL2A2, ACAN, COMP, SOX9, SOX6) (**b**) and to neurogenesis (β-TUBULIN III and NESTIN) (**c**) in NP-MSCS and NP-MSCS-N cells. For each marker, the gene expression ratio was represented as fold change with respect to undifferentiated NP-MSCs (expressed equal to 1). Data reported (mean ± SEM) are representative of three experiments; $*p < 0.05$

Analysis by Confocal Microscopy of the Expression of Neural and Neuronal-Specific Protein

The presence of neural differentiation markers was evaluated by means of confocal microscopy. The control and the differentiated NP-MSCS-N cells were fixed and stained after 10 days of culture. Compared with undifferentiated cells, the differentiation process of NP-MSCS-N seems to induce increased levels of cytosolic proteins β-TUBULIN III, MAP-2, GAP-43, and ENOLASE-2. Interestingly, NESTIN appeared increased only in a percentage of the analyzed population (Fig. 6).

Analysis by SEM and TEM of the Effects of Neural Differentiation on the Structure of NP-MSCs

SEM images of NP-MSCs showed a flat morphology and a homogeneous size (Fig. 7a). In contrast, besides the cells that maintain the undifferentiated morphology, NP-MSCs-N showed the presence of small, rounded, and fusiform cells that form clumps (Fig. 7b, c) resembling to those formed by primary hippocampal neuron in culture (Ojovan et al. 2014). TEM analysis identified elongated processes (Fig. 7d) containing orientated cytoskeletal elements. Size of the cytoskeletal elements is compatible with microtubules (arrow) and intermediate filaments (arrowhead) (Fig. 7e). Furthermore, we noted the presence of dense core vesicles likely ascribed to lipid droplet or lipofuscin (Fig. 7f).

Analysis of the Intracellular Calcium Variations

NP-MSCs before and after neural differentiation were analyzed for intracellular calcium homeostasis. At first, cells were recorded for a period of 300 s (5 min) in absence of extracellular stimuli to verify the presence of spontaneous intracellular calcium oscillations. As reported in the graphs in Fig. 8a, b, both undifferentiated (NP-MSCs) and differentiated (NP-MSCs-N) cells did not show spontaneous intracellular calcium oscillation. Moreover, no induction in intracellular calcium increase was obtained when the cells were stimulated in the presence of depolarizing agent such as 50 mM KCl (Fig. 8c, d).

Discussion

MSCs derived from non-degenerate human NP have been isolated, characterized, and induced toward neural precursor differentiation.

The features of MSCs, such as the ability to differentiate into multiple lineages, to migrate toward injured tissue, and to secrete factors identified to be important in tissue repair, attracted the attention of many researches involved in regenerative medicine, including a wide range of neurological diseases (Stoltz et al. 2015).

At present, it is unclear whether MSCs isolated from different tissue sources have similar therapeutic potentials, and so, it is necessary to verify the real ability of mesenchymal stem cells to give rise to functional adult somatic cells like neurons (Ikebe and Suzuki 2014; Bara et al. 2014).

Among the numerous adult sources, particular attention has been given to the nucleus pulposus since it may be considered a postembryonic vestige of the notochord that drives the neurulation, organizing the sequential events that lead to the development of the neural tube. Undifferentiated cells derived

Fig. 5 Analysis of the expression of NESTIN, ENOLASE-2, SNAP25, and VAMP2. Western blot and densitometric analyses of NESTIN, ENOLASE-2, SNAP25, and VAMP2, in a representative of the three performed experiments. Densitometric analyses of the immunoreactive bands is quantified as ratio between band relative to NESTIN, ENOLASE-2, SNAP25, VAMP2, and β-ACTIN in corresponding samples, revealed by arbitrary units. Data are expressed as a mean ± SD from analyses performed on NP-MSCs and NP-MSCs-N. $*p < 0.05$
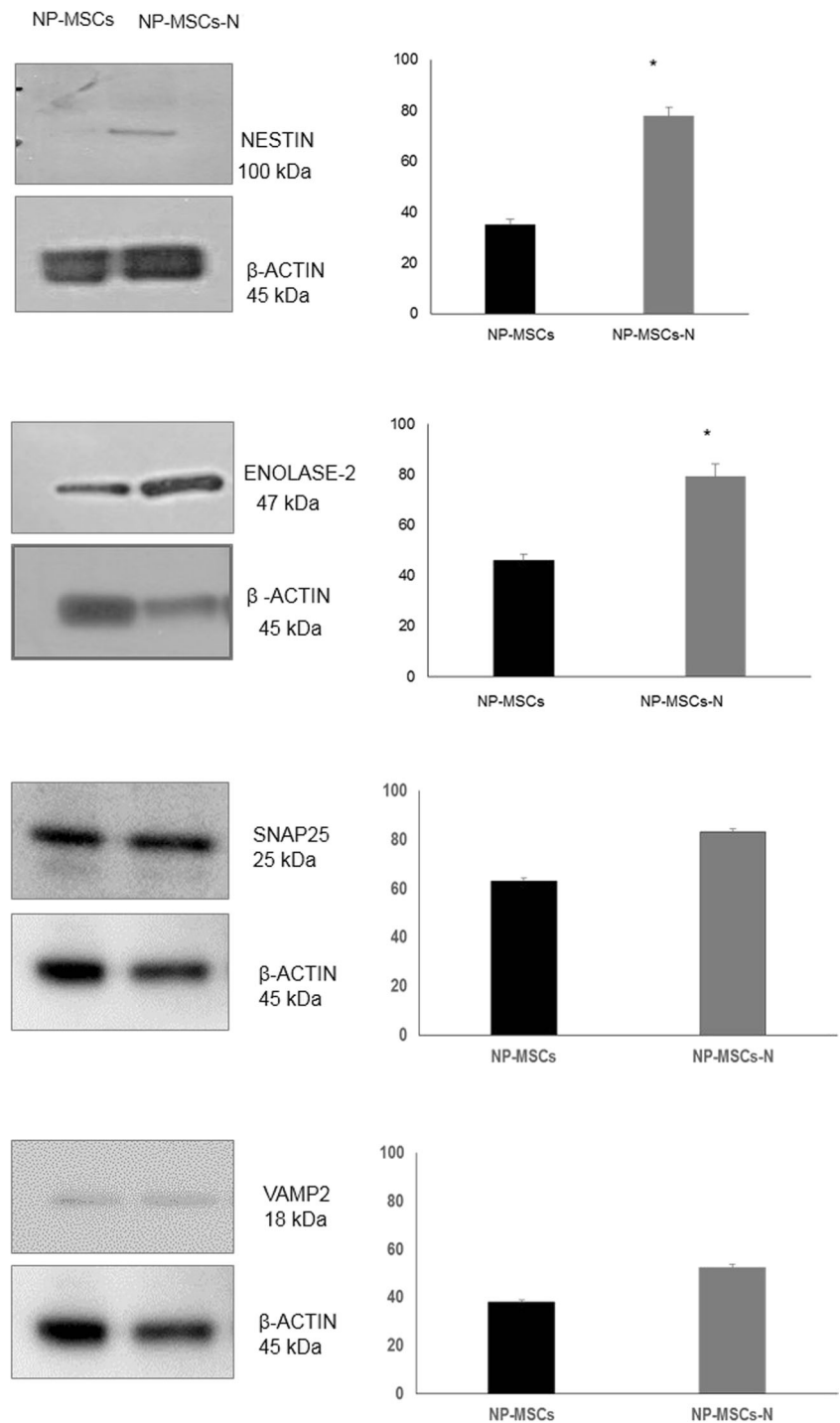

from it may preserve a major aptitude to differentiate toward neuronal lineage.

This study explored the ability of MSCs, derived from the non-degenerate nucleus pulposus tissue, to differentiate into neural-like stem cells and give rise to neural-like precursors. During the characterization, AF-MSCs were used as a control and for comparative purpose. NP-MSCs, derived from five

patients, showed a morphology, immunophenotypic pattern, and growth rate similar to those of AF-MSCs.

Among the expression of stemness genes, NP-MSCs showed higher level of OCT4 compared with AF-MSCs; OCT4 constitutes the core regulatory network that suppresses differentiation-associated genes, thereby maintaining pluripotency of the cells. This pluripotent factor is a
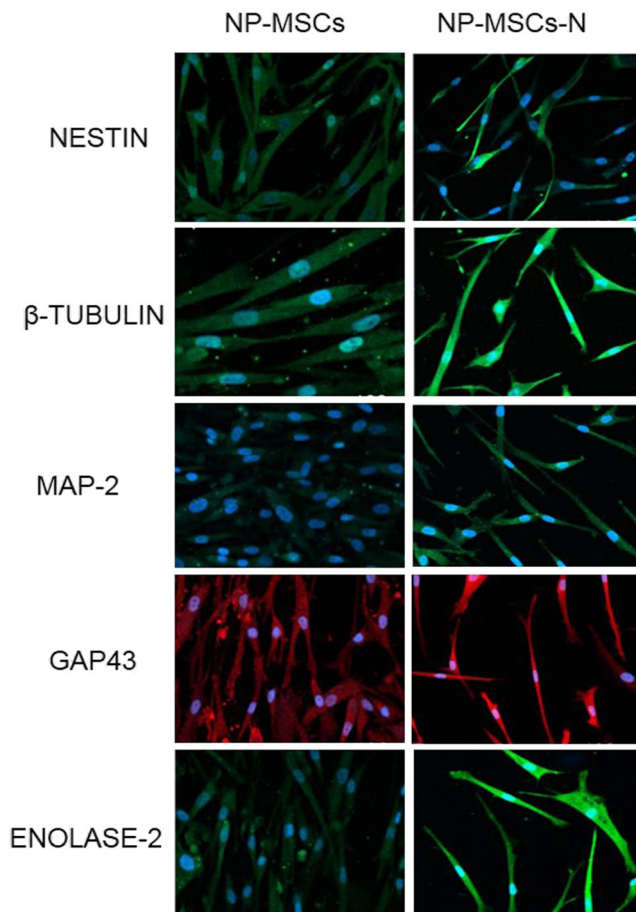
Fig. 6 Confocal microscopy. Representative images of NP-MSCs cells before (NP-MSCs) and after neuronal differentiation (NP-MSCs-N). Green fluorescence emission: NESTIN, β-TUBULIN III (β-TUBULIN), microtubule-associated protein 2 (MAP-2), and neuronal-specific enolase (ENOLASE-2); red fluorescence: emission growth-associated protein 43 (GAP-43). All the images are counterstained for nuclei with DAPI. Magnification ×400

transcription factor essential to pluripotent and self-renewing phenotypes (Nichols et al. 1998).

NP-MSCs were able to differentiate into chondrogenic and osteogenic lineages but failed to differ into adipogenic lineage. The inability of NP-MSCs to differentiate toward adipogenic lineage is in accordance with the data previously reported by Blanco et al. (2010) and Shen et al. (2015). The age of the patients seems to be the factor that influenced the adipogenic differentiation potential of MSCs isolated from NP: cells from cases with the average age lower than 20 years are able to differentiate into adipocyte (Blanco et al. 2010; Shen et al. 2015). On the other hand, cells derived from patients older than 20 years failed the differentiation toward adipogenic lineage. Since the average age in this case is 54 ±4 years, the failure in adipogenic differentiation is in agreement with the pre-existing literature. The expression of genes related to chondrogenic tissue was tested; NP-MSCs expressed detectable levels of COL1A1, COL2A2, ACAN, COMP, SOX9, and SOX6. The expression, at low level, of genes specific of the origin tissue is often observed in MSCs (Secco et al. 2009).

After stemness state identification for isolated cells, NP-MSCs were induced toward neuronal differentiation for 10 days by using a neural differentiation medium.

Neuronal differentiated NP-MSCs (NP-MSCs-N) changed their morphology, proliferation rate, and the expression of selected genes. Indeed, cells exhibit the formation of neurite-like extension and the proliferation rate decreased; both these observations suggest a real induction toward differentiated cells.

Regarding expression profile of genes related to stemness, NP-MSCs-N overexpressed SOX2 that is one of the critical factors that control pluripotency, neural differentiation, and the maintenance of neural progenitor's stem cells (Graham et al. 2003; Bylund et al. 2003). Looking to the expression of genes related to chondrogenesis, COMP, SOX6, and SOX9 were downregulated. COMP and SOX9 are key factors in the activation of chondrogenesis, and SOX6 is closely related to the function of SOX9. Their reduction is in line with the induction of the neuronal differentiation. NP-MSCs-N showed an increase in the expression of COL2A1, compared to the undifferentiated cells. This effect is probably due to the presence of IGF1 in the neural medium; IGF1 increased type II collagen synthesis by a transcriptional control mechanism involving a 715-bp region within the COL2A1 first intron-specific enhancer (Renard et al. 2012).

Since it is reported that the ability to form neurosphere is an almost exclusive feature of neural stem/progenitor cells, this capacity was tested in NP-MSCs-N. Differentiated cells were able to continue cell division and generate non-adherent spherical clusters of cells, commonly referred to as neurosphere (Bez et al. 2003). NP-MSCs undergoing to neuronal differentiation lost their original mesenchymal morphology to progressively acquire a neuronal phenotype. To achieve the new phenotype, proteins involved in the cytoskeleton rearrangement for axon guidance and in synaptic vesicle exocytosis are expressed by differentiating cells. To address this issue, the expression of selected proteins was tested.

VAMP2 and SNAP25 are components of soluble *N*-ethylmaleimide-sensitive fusion attachment protein receptors (SNARE) complex which is involved in the vesicle fusion for the neurotransmitter release. In the developing nervous system, they are important for neurite outgrowth and transformation of the growth cone into the mature synapse (Hepp and Langley 2001). Their expression was improved after neural differentiation without reaching a statistically significant increase compared to control cells; this failure may indicate as our treated cells are initiating the differentiation toward neuronal cells without reaching a mature phenotype characterized by these markers.
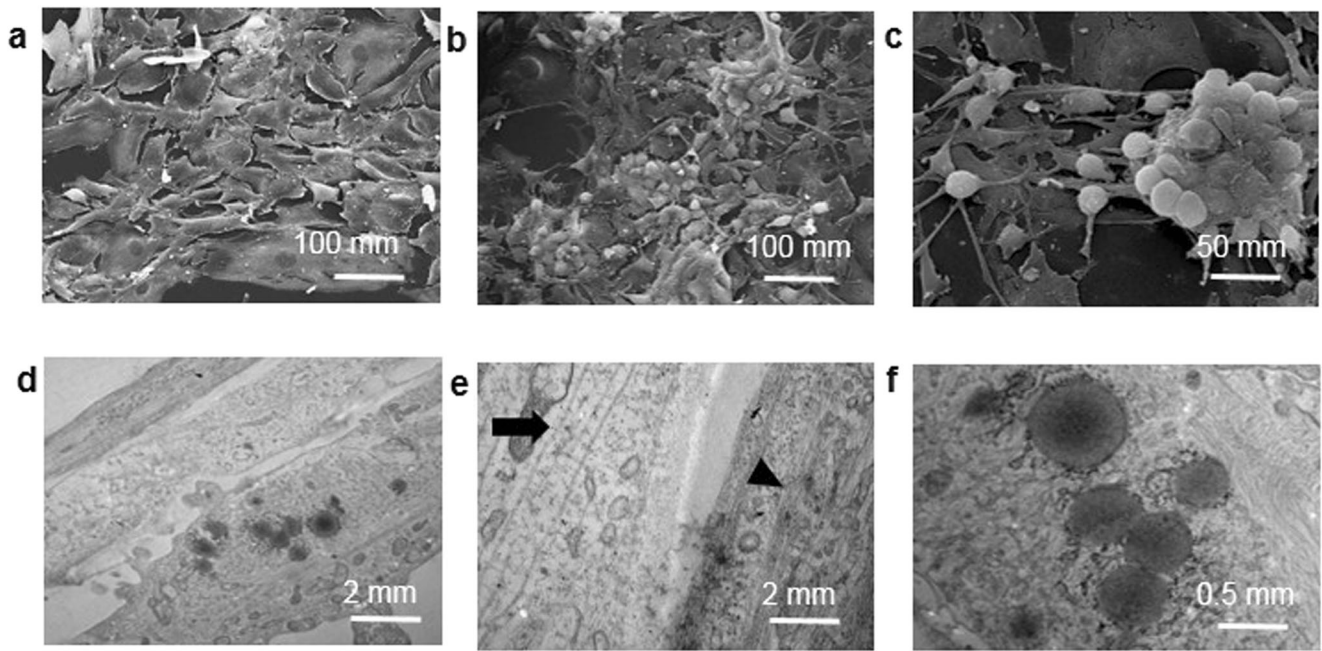
Fig. 7 Electron microscopy. SEM images of control NP-MSCs cells (**a**) and neuronal differentiated cells (**b**, **c**). **d** TEM images of NP-MSCs-N; at greater magnification, it is possible to note microtubule and intermediate filaments (**e**) and lipidic droplets (**f**). Images are representative of three independent experiments
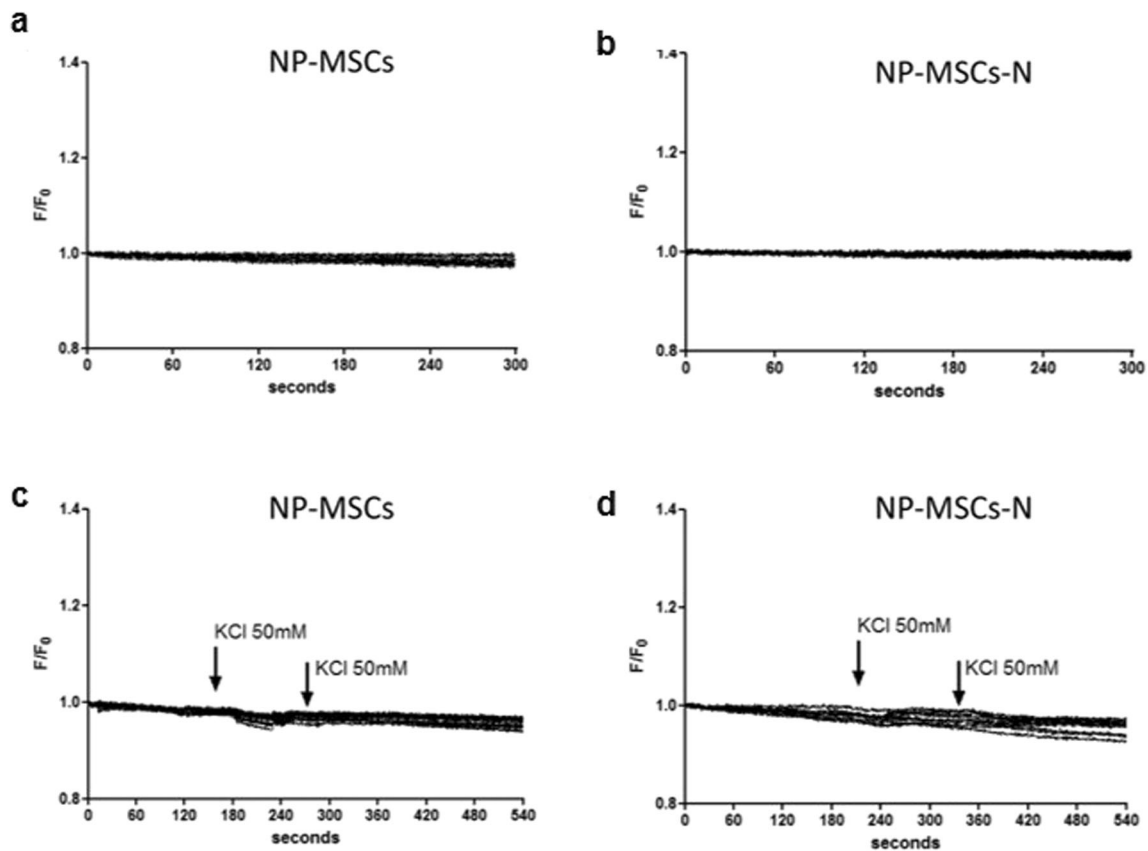
Fig. 8 Intracellular calcium measurements. Representative traces of spontaneous intracellular calcium oscillations in undifferentiated NP-MSCs cells (NP-MSCs) (**a**) or neuronal differentiated NP-MSC cells (NP-MSCs-N) (**b**). Representative recordings of KCl 50 mM depolarization evoked in control NP-MSCs (**c**) or neuronal differentiated NP-MSCs cells (NP-MSCs-N) (**d**)

In addition, the expression of proteins referred to cytoskeleton rearrangement, such as NESTIN, β-TUBULIN III, GAP43, MAP-2, and ENOLASE-2, was evaluated. Results obtained by Western blot and confocal microscopy revealed that differentiated NP-MSCs expressed higher level of these proteins than control cells. In detail, the statistically significant increase observed at mRNA level for NESTIN was confirmed at protein level by Western blot. NESTIN is an intermediate filament protein that is known as a neural stem/progenitor cell marker. GAP-43 is normally expressed at high levels in neuronal growth cones during development (Rosskothen-Kuhl and Illing 2014) and is considered a crucial component of the axon and presynaptic terminal.

β-TUBULIN III is a microtubule element of the tubulin family found almost exclusively in neurons involved in axon guidance and maintenance (Avwenagha et al. 2003).

MAP-2 is involved in microtubule assembly, which is an essential step in neurogenesis, specifically in dendrites, implicating a role in determining and stabilizing dendritic shape during neuron development (Harada et al. 2002). Finally, ENOLASE-2 (the neural specific enolase) exerts neurotrophic activity regulating neuronal growth, differentiation, and survival.

The overexpression of these proteins correlates with the results from TEM and SEM, where cells display morphological features typical of the neural progenitors, in particular orientated cytoskeletal elements with a size compatible with microtubules and intermediate filaments. Even if morphological and biochemical analyses seem to indicate that NP-MSCs acquire a neuronal phenotype, functional analysis failed to demonstrate the presence of spontaneous intracellular calcium oscillations or the voltage-dependent channels. This aspect could be indicative of an incomplete differentiation that in our experimental conditions activates only a part of the genetic program able to bring the cells to full neuronal features.

Conclusions

It is possible to isolate MSCs from human NP-MScs that can be induced toward neural differentiation; after induction, even if there are morphological and biochemical changes, cells do not acquire the functionality of mature neurons, indicating an incomplete differentiation.

Even if further studies will be necessary to elucidate the exact differentiation protocols, the aptitude of NP-MSCs to differentiate into neural precursor cells can expand the research focused in the identification of stem cells sources that are able to differentiate into functional nervous system-specific cells.

References

Alexanian AR, Maiman DJ, Kurpad SN, Gennarelli TA (2008). In vitro and in vivo characterization of neurally modified mesenchymal stem cells induced by epigenetic modifiers and neural stem cell environment. Stem Cells Dev 17:1123–1130. https://doi.org/10.1089/scd.2007.0212.

Avwenagha O, Campbell G, Bird MM (2003) Distribution of GAP-43, beta-III tubulin and F-actin in developing and regenerating axons and their growth cones in vitro, following neurotrophin treatment. J Neurocytol 32:1077–1089. https://doi.org/10.1023/B:NEUR.0000021903.24849.6c

Bara JJ, Richards RG, Alini M, Stoddart MJ (2014) Concise review: bone marrow-derived mesenchymal stem cells change phenotype following in vitro culture: implications for basic research and the clinic. Stem Cells 32:1713–1723. https://doi.org/10.1002/stem.1649

Bez A, Corsini E, Curti D, Biggiogera M, Colombo A, Nicosia RF, Pagano SF, Parati EA (2003) Neurosphere and neurosphere-forming cells: morphological and ultrastructural characterization. Brain Res 993:18–29

Bianco P, Robey PG, Simmons PJ (2008) Mesenchymal stem cells: revisiting history, concepts, and assays. Cell Stem Cell 2:313–319. https://doi.org/10.1016/j.stem.2008.03.002

Blanco JF, Graciani IF, Sanchez-Guijo FM, Muntión S, Hernandez-Campo P, Santamaria C, Carrancio S, Barbado MV, Cruz G, Gutierrez-Cosío S, Herrero C, San Miguel JF, Briñon JG, del Cañizo MC (2010) Isolation and characterization of mesenchymal stromal cells from human degenerated nucleus pulposus: comparison with bone marrow mesenchymal stromal cells from the same subjects. Spine (Phila Pa 1976) 35:2259–2265. https://doi.org/10.1097/BRS.0b013e3181cb8828

Bylund M, Andersson E, Novitch BG, Muhr J (2003) Vertebrate neurogenesis is counteracted by Sox1-3 activity. Nat Neurosci 6:1162–1168. https://doi.org/10.1038/nn1131

Caprara GA, Morabito C, Perni S, Navarra R, Guarnieri S, Mariggiò MA (2016) Evidence for altered Ca2+ handling in growth associated protein 43-knockout skeletal muscle. Front Physiol 7:493. https://doi.org/10.3389/fphys.2016.00493

Casarosa S, Bozzi Y, Conti L (2014) Neural stem cells: ready for therapeutic applications? Mol Cell Ther 2:31. https://doi.org/10.1186/2052-8426-2-31

Dominici M, Le Blanc K, Mueller I, Slaper-Cortenbach I, Marini F, Krause D, Deans R, Keating A, Dj P, Horwitz E (2006) Minimal criteria for defining multipotent mesenchymal stromal cells. The International Society for Cellular Therapy position statement. Cytotherapy 8:315–317. https://doi.org/10.1080/14653240600855905

Foudah D, Monfrini M, Donzelli E, Niada S, Brini AT, Orciani M, Tredici G, Miloso M (2014, 2014) Expression of neural markers by undifferentiated mesenchymal-like stem cells from different sources. J Immunol Res:987678. https://doi.org/10.1155/2014/987678

Friedenstein AJ, Petrakova KV, Kurolesova AI, Frolova GP (1968) Heterotopic of bone marrow. Analysis of precursor cells for osteogenic and hematopoietic tissues. Transplantation 6:230–247

Graham V, Khudyakov J, Ellis P, Pevny L (2003) SOX2 functions to maintain neural progenitor identity. Neuron 39:749–765

Harada A, Teng J, Takei Y, Oguchi K, Hirokawa N (2002) MAP2 is required for dendrite elongation, PKA anchoring in dendrites, and proper PKA signal transduction. J Cell Biol 158:541–549. https://doi.org/10.1083/jcb.200110134

Hepp R, Langley K (2001) SNAREs during development. Tissue Res 305:247–253

Ikebe C, Suzuki K (2014) Mesenchymal stem cells for regenerative therapy: optimization of cell preparation protocols. Biomed Res Int 2014:951512. https://doi.org/10.1155/2014/951512

Lazzarini R, Olivieri F, Ferretti C, Mattioli-Belmonte M, Di Primio R, Orciani M (2014) mRNAs and miRNAs profiling of mesenchymal stem cells derived from amniotic fluid and skin: the double face of the coin. Cell Tissue Res 355:121–130. https://doi.org/10.1007/s00441-013-1725-4

Madrigal M, Rao KS, Riordan NH (2014) A review of therapeutic effects of mesenchymal stem cell secretions and induction of secretory modification by different culture methods. J Transl Med 12:260. https://doi.org/10.1186/s12967-014-0260-8

Mariotti C, Lazzarini R, Nicolai M, Saitta A, Orsini E, Orciani M, Di Primio R (2015). Comparative study between amniotic-fluid mesenchymal stem cells and retinal pigmented epithelium (RPE) stem cells ability to differentiate towards RPE cells. Cell Tissue Res 362:21–31. https://doi.org/10.1007/s00441-015-2185-9.

Morabito C, Guarnieri S, Fanò G, Mariggiò MA (2010) Effects of acute and chronic low frequency electromagnetic field exposure on PC12 cells during neuronal differentiation. Cell Physiol Biochem 26:947–958. https://doi.org/10.1159/000324003

Nichols J, Zevnik B, Anastassiadis K, Niwa H, Klewe-Nebenius D, Chambers I, Schöler H, Smith A (1998) Formation of pluripotent stem cells in the mammalian embryo depends on the POU transcription factor Oct4. Cell 95:379–391

Ojovan SM, McDonald M, Rabieh N, Shmuel N, Erez H, Nesladek M, Spira ME (2014) Nanocrystalline diamond surfaces for adhesion and growth of primary neurons, conflicting results and rational explanation. Front Neuroeng 7:17. https://doi.org/10.3389/fneng.2014.00017

Orciani M, Davis S, Appolloni G, Lazzarini R, Mattioli-Belmonte M, Ricciuti RA, Boscaro M, Di Primio R, Arnaldi G (2015) Isolation and characterization of progenitor mesenchymal cells in human pituitary tumors. Cancer Gene Ther 222:9–16. https://doi.org/10.1038/cgt.2014.63.

Orciani M, Mariggiò MA, Morabito C, Di Benedetto G, Di Primio R (2010) Functional characterization of calcium-signaling pathways of human skin-derived mesenchymal stem cells. Skin Pharmacol Physiol 23:124–132. https://doi.org/10.1159/000270383

Pittenger MF, Mackay AM, Beck SC, Jaiswal RK, Douglas R, Mosca JD, Moorman MA, Simonetti DW, Craig S, Marshak DR (1999) Multilineage potential of adult human mesenchymal stem cells. Science 284:143–147

Renard E, Porée B, Chadjichristos C, Kypriotou M, Maneix L, Bigot N, Legendre F, Ollitrault D, De Crombrugghe B, Malléin-Gérin F, Moslemi S, Demoor M, Boumediene K, Galéra P (2012) Sox9/Sox6 and Sp1 are involved in the insulin-like growth factor-I-mediated upregulation of human type II collagen gene expression in articular chondrocytes. J Mol Med (Berl) 90:649–666. https://doi.org/10.1007/s00109-011-0842-3

Rosskothen-Kuhl N, Illing RB (2014) Gap43 transcription modulation in the adult brain depends on sensory activity and synaptic cooperation. PLoS One 9:e92624. https://doi.org/10.1371/journal.pone.0092624

Sagar R, Walther-Jallow L, David AL, Götherström C, Westgren M (2018) Fetal mesenchymal stromal cells: an opportunity for prenatal cellular therapy. Curr Stem Cell Rep 4:61–68. https://doi.org/10.1007/s40778-018-0118-8

Sana J, Zambo I, Skoda J, Neradil J, Chlapek P, Hermanova M, Mudry P, Vasikova A, Zitterbart K, Hampl A, Sterba J, Veselska R (2011) CD133 expression and identification of CD133/nestin positive cells in rhabdomyosarcomas and rhabdomyosarcoma cell lines. Anal Cell Pathol (Amst) 34:303–318. https://doi.org/10.3233/ACP-2011-0018.

Secco M, Moreira YB, Zucconi E, Vieira NM, Jazedje T, Muotri AR, Okamoto OK, Verjovski-Almeida S, Zatz M (2009) Gene expression profile of mesenchymal stem cells from paired umbilical cord units: cord is different from blood. Stem Cell Rev 5:387–401. https://doi.org/10.1007/s12015-009-9098-5

Shen Q, Zhang L, Chai B, Ma X (2015) Isolation and characterization of mesenchymal stem-like cells from human nucleus pulposus tissue. Sci China Life Sci 58:509–511. https://doi.org/10.1007/s11427-015-4839-y

Shyu WC, Chen CP, Lin SZ, Lee YJ, Li H (2007) Efficient tracking of non-iron-labeled mesenchymal stem cells with serial MRI in chronic stroke rats. Stroke 38:367–374. https://doi.org/10.1161/01.STR.0000254463.24655.14

Stoltz JF, de Isla N, Li YP, Bensoussan D, Zhang L, Huselstein C, Chen Y, Decot V, Magdalou J, Li N, Reppel L, He Y (2015) Stem cells and regenerative medicine: myth or reality of the 21th century. Stem Cells Int 2015:734731:1–19. https://doi.org/10.1155/2015/734731

Trueman RC, Klein A, Lindgren HS, Lelos MJ, Dunnett SB (2013) Repair of the CNS using endogenous and transplanted neural stem cells. Curr Top Behav Neurosci 15:357–398. https://doi.org/10.1007/7854_2012_223

Uccelli A, Morando S, Bonanno S, Bonanni I, Leonardi A, Mancardi G (2011) Mesenchymal stem cells for multiple sclerosis: does neural differentiation really matter? Curr Stem Cell Res Ther 6:69–72

Uccelli A, Moretta L, Pistoia V (2008) Mesenchymal stem cells in health and disease. Nat Rev Immunol 8:726–736. https://doi.org/10.1038/nri2395

Ullah I, Subbarao RB, Rho GJ (2015) Human mesenchymal stem cells—current trends and future prospective. Biosci Rep 35 e00191:1–18. https://doi.org/10.1042/BSR20150025

Zannettino AC, Paton S, Arthur A, Khor F, Itescu S, Gimble JM, Gronthos S (2008) Multipotential human adipose-derived stromal stem cells exhibit a perivascular phenotype in vitro and in vivo. J Cell Physiol 214:413–421. https://doi.org/10.1002/jcp.21210

Zhao C, Deng W, Gage FH (2008). Mechanisms and functional implications of adult neurogenesis. Cell 132:645–660. https://doi.org/10.1016/j.cell.2008.01.033, Mechanisms and Functional Implications of Adult Neurogenesis.